Appl Phys B (2009) 94: 215–219
DOI 10.1007/s00340-008-3312-z

Applied Physics B
Lasers and Optics

Laser emission in Nd:YVO_4 channel waveguides at 1064 nm

M.E. Sánchez-Morales · G.V. Vázquez · E.B. Mejía · H. Márquez · J. Rickards · R. Trejo-Luna

Received: 7 July 2008 / Revised version: 10 October 2008 / Published online: 28 November 2008

Abstract In this work, we report 1064 nm laser emission in Nd:YVO_4 channel waveguides fabricated by carbon implantation. Typical threshold pump powers (∼808 nm) were ≥45 mW. Maximum conversion efficiency was 11.5% (29.6% slope efficiency), and up to 9 mW of signal was delivered. Sample lengths of 4 mm were sufficient to completely absorb the pump power. The special spectral characteristics of this material such as broad absorption band and superior cross sections compared to the YAG crystal makes it suitable for developing compact sources to be integrated in optoelectronic devices.

PACS 42.82.Et · 42.70.Hj · 42.60.-v

1 Introduction

Nd^{3+}-doped lasers are among the most studied and commercialized solid state lasers. The four-level nature of the $^4F_{3/2} \rightarrow {}^4I_{11/2}$ transition permits a relatively easy achievement of population inversion for oscillation. Earliest systems were Nd^{3+}-doped bulk crystals pumped by non-coherent white-light sources that delivered most of the optical power in bands that are not absorbed by the Nd^{3+} ions. Then, in addition to the poor electrical-to-optical conversion efficiencies of the lamps, the low optical-to-optical conversion efficiency of these lasers resulted, in the best cases, in 3% overall efficiencies [1]. With the rapid development and commercialization of pump laser diodes, these systems scaled up to around 50% efficiency (optical-to-optical) and were more compact and robust [2]. The development of doped waveguides allowed the confinement of very narrow beams, ensuring in this way a total overlapping of pump and signal over long distances of laser material. The Nd:YAG crystal is among the natural candidates for doped waveguide lasers. It has been a high-quality system that is robust, and its efficiency scaled up [3–5]. Other laser materials have also been investigated such as the YVO_4, in which the Nd^{3+} ions present some more advantageous spectral characteristics such as broader (up to six times) absorption bands and also superior (up to four times) absorption and emission cross sections compared to YAG [6].

The ion implantation technique has proved to generate both planar and channel waveguides not only in these crystals but in more than 60 different materials [7, 8]. The implanted ions cause nuclear collisions which generally reduce the physical density of the lattice at the end of the ion trajectory; hence a region of lower refractive index is formed. In this way, a waveguide is produced between this low-density region and the surface. Our fabrication capabilities of both planar and channel waveguides in Nd:YVO_4 by the ion implantation technique [9, 10] had motivated us to achieve the results reported here. We have obtained laser oscillation at 1064 nm by pumping at around 808 nm in several channels

M.E. Sánchez-Morales
Departamento de Ciencias Básicas, Centro Universitario la Ciénaga-Universidad de Guadalajara, Avenida Universidad 1115, Linda Vista, 47810 Ocotlán, Jalisco, Mexico

G.V. Vázquez (✉) · E.B. Mejía
Centro de Investigaciones en Óptica, Loma del Bosque 115, Lomas del Campestre, 37150 León, Guanajuato, Mexico
e-mail: gvvazquez@cio.mx
Fax: +52-477-4414209

H. Márquez
Departamento de Óptica, CICESE, Km 107 Carr. Tijuana-Ensenada, 22860 Ensenada, B.C., Mexico

J. Rickards · R. Trejo-Luna
Instituto de Física, Universidad Nacional Autónoma de México, Apartado Postal 20364, 01000 México D.F., Mexico

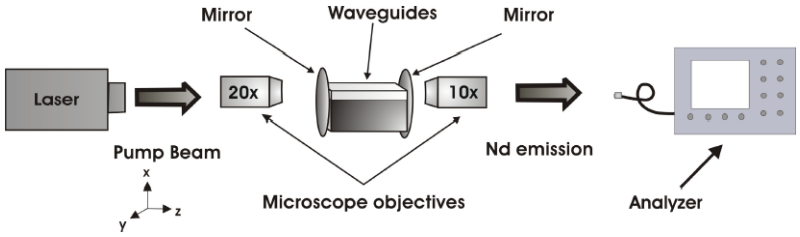

Fig. 1 Experimental arrangement to assess laser performance in the channel waveguides

of a short, 4-mm sample. The system was characterized regarding efficiencies for three cavity configurations, and the output intensity profile was also obtained. Potential applications such as on-chip micro lasers are proposed, and improvements are suggested.

2 Experimental methods

The channel waveguides were fabricated on an a-cut 1 at.%-doped Nd:YVO_4 crystal by the ion implantation technique using carbon ions at an energy of 7 MeV and a dose of 8.0×10^{14} ions/cm^2 [10, 11]. Standard microlithography was used to make the mask apertures of 20 μm width with 40 μm spacing between them on an aluminum layer deposited on the vanadate crystal. The waveguides obtained have 4 mm length with a cross-section area of $\sim 5 \times 20$ μm^2 and spacing of $\sim$40 μm. Previously to the laser emission studies, the propagation loss in the waveguides was reduced. For this purpose, an annealing process was carried out using an electrical furnace at 350 °C in open atmosphere (according to results of [11]). The annealing time was increased by two-hour periods up to 26 hours.

The end-coupling method was used to measure the propagation losses, where light coming from a He–Ne laser (633 nm) was coupled to the waveguides using a 40× microscope objective, and the output light was collected by a 20× microscope objective. Also, optical microscopy was used to observe the damage caused by the implanted ions in the crystal and thus identify the channel regions generated near the surface.

An experimental arrangement based on the prism-coupling technique was used to monitor the propagation modes in the waveguides, giving us the confinement properties in the x-direction. The effective refractive indices were measured with a prism coupler (Model 2010, Metricon Corporation) [11]. In order to appraise the mode confinement in both axes, we also estimated the V parameter, which depends on the refractive index at the different interfaces.

In terms of spectroscopic studies, we previously obtained the luminescence spectrum of the neodymium ions in the YVO_4 host [10]; in the present work we carried out further spectroscopic characterization measuring the Nd emission lifetime. Light from an 811-nm diode laser was modulated with a mechanical chopper and coupled into the waveguides using the end-coupling technique; the output signal was synchronously detected and averaged by a digital oscilloscope.

Figure 1 shows a scheme of the experimental setup for laser emission. A tunable Ti:Sapphire laser, whose polarization coincided with the ordinary index of the crystal in the y-direction, pumped the cavity at 808 nm through a 20× microscope objective (MO). With this polarization, the Nd^{3+} ions in the YVO_4 crystal present the highest value of stimulated emission cross-section. The crystal dimensions were 1, 6, and 4 mm for the x, y, and z coordinates respectively. The focused beam was coupled to the waveguide entrance that was in mechanical (and optical) contact with a high-reflectivity mirror (∼100% at the lasing wavelength). Low-fluorescence immersion oil was used to adhere the mirrors to the bulk crystal that contained the waveguides. We estimated a coupling efficiency of 50% as the ratio of output-to-incident power at a wavelength not absorbed by the Nd^{3+} ions. In this way, the value is given by the crystal characteristics and waveguide losses, which, as we will mention later, vary from one channel to another. Several $\sim 5 \times 20$ μm (cross section) waveguide channels lased (one at a time), and their positioning was made by using an X–Y–Z high-resolution stage. Three mirrors with reflectivities of 97%, 23.2%, and 10.5% (air–crystal interface) at the lasing wavelength were used as the output couplers (OC) of the cavity. The output signal was collected and collimated by a 10× MO, the intensity profile was characterized, its power measured with a Gentec E–O meter, and the spectrum analyzed by means of an ANDO optical spectrum analyzer with 0.01 nm of maximum resolution. The pump signal was completely absorbed, as the absorption coefficient of 1% Nd-doped YVO_4 is about 32 cm^{-1} at 808 nm, then the percentage of absorbed power for 0.2 cm length is ∼99%, and thus the output spectrum practically contained the 1064-nm alone. All experiments were realized at room temperature, and no thermal cooling of the crystal was necessary.

3 Results and discussion

The initial propagation losses were approximately 35 dB/cm; with the 26-hour annealing treatment, the losses were reduced to ∼10 dB/cm. Images obtained by optical mi-

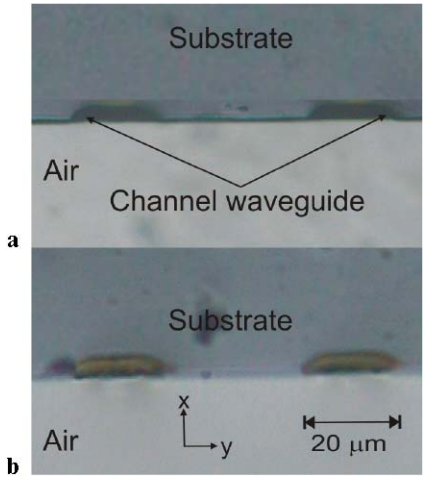

Fig. 2 Images by optical microscopy of the channel cross-section: **a** before annealing, **b** after a 26-hour annealing at 350°C in open atmosphere

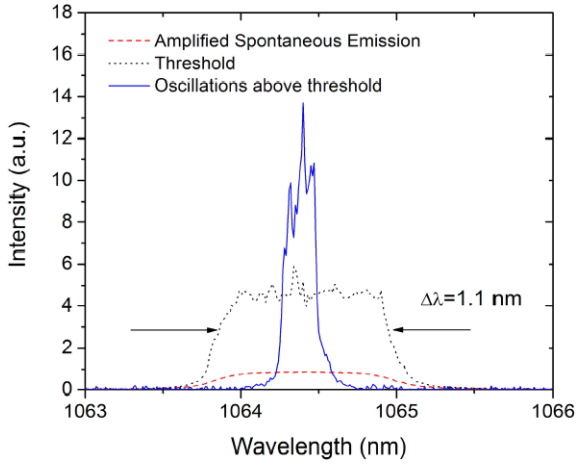

Fig. 3 Signal emission at around 1064 nm for different pump powers using the 3% OC. The *dashed*, *dotted*, and *solid curves* represent respectively the amplified spontaneous emission (ASE) at low pump power, the ASE at threshold, and the oscillations just above threshold

croscopy confirm the loss reduction as seen in the (a) non-annealed and (b) 26-hour annealed pictures in Fig. 2. Observe that the originally dark cross section view of the channels (Fig. 2a) becomes more transparent (Fig. 2b). Regarding waveguide modes, after the implantation, the waveguides confined eight ordinary modes in the x-direction [10]. At the end of the annealing, only one ordinary mode was coupled, with an effective refractive index value of around 1.9673. By taking into account the rectangular shape of the waveguide's cross section operating with polarization that coincides with the ordinary refractive index after annealing, that is 1.968 in the waveguide layer (close to the surface) and 1.9646 in the implanted region where ions are stopped, i.e., optical barrier, we have estimated the V parameter to be $V = (2\pi/\lambda)(2.5\ \mu\text{m})(1.968^2 – 1.9646^2)^{1/2} = 2.87$ at 633 nm, 2.0 for 808 nm, and 1.4 (1064 nm) for the vertical coordinate. Refractive index values were obtained using a multi-layer approximation. The V parameter was also estimated for the horizontal dimension giving ~8.0 for 808 nm and ~6.1 for 1064 nm [12]. Then, the waveguide is single-mode in the vertical direction and multimode in the horizontal direction at the pump and lasing wavelength. In fact, an additional objective of the annealing treatment was to reduce the number of guided modes as the induced index changes are decreased for long annealing times [13]; this is of advantage for laser operation, as it would be desirable to obtain a single transverse mode. Thus, the multimode operation in the horizontal direction is one of the important parameters to adjust for future work because beam shaping is necessary for non-square or non-circular beams. For this purpose, our efforts will be focused on optimizing the implanted ion dose and fabricating narrower waveguides. Indeed, thinner waveguides have been fabricated on this material by oxygen implantation, and they showed single-mode operation [14].

The luminescence of the neodymium ions in the YVO_4 channels was characterized in a previous work [10], where it was shown that the emission spectrum at 1064 nm coincided with that from the bulk crystal. The lifetime measured in this work was the same in the waveguides and in the substrate, 90 μs. These results confirm that the spectroscopic characteristics of Nd^{3+} in YVO_4 are preserved in the channel waveguides.

When the waveguides together with the mirrors formed the laser cavity and it was pumped, laser oscillation was achieved and characterized as described below. Figure 3 shows the signal emitted at different pump powers when using the 3% OC. The dashed curve is the amplified spontaneous emission (ASE) before reaching laser threshold, and the dashed-dotted line corresponds to the ASE plus oscillations just above threshold. Note the emission along the 1063.7–1065.2 nm range. When further increasing the pump power, the emission spectrum started to become narrower (see the solid curve) until a single sharp peak was established at 1064.4 nm with a full width at half maximum (FWHM) $\Delta\lambda$ of 0.16 nm, as shown in Fig. 4. Nonuniformity in the cross-section shape along the waveguides is believed to be responsible of a nonsymmetric intensity pattern delivered by the system (see the inset of Fig. 4). Under a more controlled process, the profile might be more symmetric.

Figure 5 contains the dependence of 1064-nm output power on the 808 nm absorbed pump power for one of the channels that better performed. With the 3% transmission OC mirror (curve in circles), the threshold for oscillation was ~45 mW, and the maximum optical conversion efficiency, as expected, was quite low (0.7% with a slope of 1.3%). Hence, the maximum conversion efficiency, accounting for intra-cavity signal, may be estimated as the intra-cavity signal (the quotient of maximum delivered power to

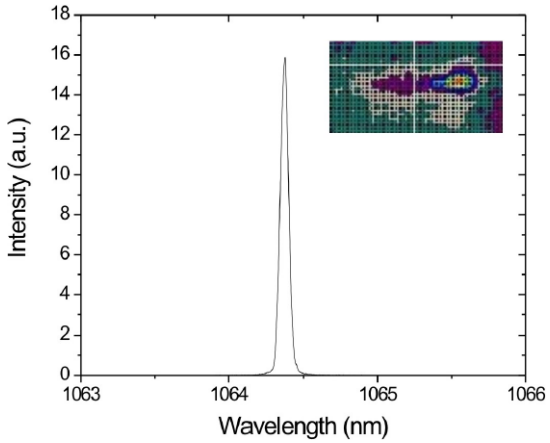

Fig. 4 Typical laser emission spectrum at the highest pump powers and the intensity profile of the beam delivered (*inset*), where the white lines only represent the center of the CCD camera. The 3% OC was used

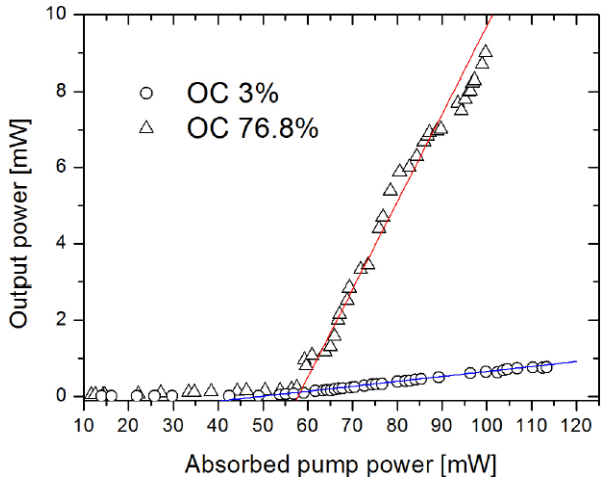

Fig. 5 Dependence of output power on the absorbed pump power using the 3% (*circles*) and the 77% (*triangles*) transmission output couplers

mirror transmission, i.e., 0.75 mW/0.03 = 25 mW) over the absorbed pump power (25 mW/110 mW = 0.227), giving 22.7%. Because the quantum efficiency is (808.4/1064.4 ≈ 0.76) 76%, there is still a considerable amount of work that has to be done to get close to the theoretical limit of the system. Issues such as material losses introduced during the waveguide fabrication and optimal ion concentrations have to be addressed in future work. The curve formed by triangles corresponds to the OC with a transmission of ∼77%; up to 9 mW output power was obtained with a maximum efficiency of 9% and a slope of 23.8%. Under these conditions, the pump threshold was 55–58 mW, and the maximum conversion efficiency (accounting for intra-cavity signal) was 39%. The increase in slope efficiency and pump threshold is reasonable considering the theoretical analysis presented below, where both parameters depend on the OC reflectivity.

In a four-level laser, the threshold pump power for oscillation (P_{th}) is given by [15]

$$P_{\text{th}} = \frac{hc}{\lambda_p}\frac{1}{\eta\sigma_e\tau}\frac{\delta}{2}A_{\text{eff}}, \tag{1}$$

and the slope efficiency (Φ) can be estimated by

$$\Phi = \eta\frac{1-R_2}{\delta}\frac{\lambda_p}{\lambda_s}, \tag{2}$$

where h is the Planck's constant, c is the speed of light in the vacuum, σ_e is the stimulated emission cross section, τ is the fluorescence lifetime, A_{eff} is the effective pump area, λ_s and λ_p are the signal and pump wavelengths, respectively, η is the fraction of absorbed photons that contribute to the population of the $^4F_{3/2}$ metastable state ($\eta = 1$), and R_2 is the output mirror reflectivity at the signal wavelength. The round-trip cavity exponential factor δ, which depends on the propagation loss coefficient (α), the cavity length (l), and the input (R_1) and output (R_2) mirror reflectivity, is defined as

$$\delta = 2\alpha l - \ln(R_1 R_2). \tag{3}$$

Observe from (1) to (3) that in good agreement with the experimental results, by reducing R_2, both the threshold pump power and the slope efficiency are increased.

In a different experimental session we attempted laser oscillation without a physical mirror as the OC, in such a way that the output coupling was increased to 89.5% (formed by the air–crystal interface). Although with less accuracy, the maximum conversion efficiency for extracted power was estimated to be the highest (∼11.5%), with a slope efficiency of 29.6% and a maximum intra-cavity conversion efficiency of 12.5%. This is illustrated by the curve fitted to the data measurements of Fig. 6. Power instabilities that produced the scattered data points are attributed to the lower Q-factor of the cavity. The most important aspect to be noticed is the high slope efficiency (∼29.6%) without the need of a physical mirror, which is advantageous when fabricating microlasers. The loss estimations presented below allow us to suspect that the waveguide that oscillated in this session was probably another one and thus it is not possible to make a quantitative comparison with the previous results.

The waveguide propagation loss coefficient (α) was calculated using the results for the slope efficiency, reflectivity, and (2) and (3). From Fig. 5 we know that the slope efficiencies are 0.0133 and 0.238 with the 3% and the 77% transmission output couplers, respectively, and then we estimated the propagation loss coefficients and obtained ∼8.6 and ∼5.2 dB/cm, respectively. We believe that the real value is closer to 8.6 dB/cm because the threshold value and the slope efficiency are more accurate in the first case (i.e., using the 3% transmission OC). In the case where no physical

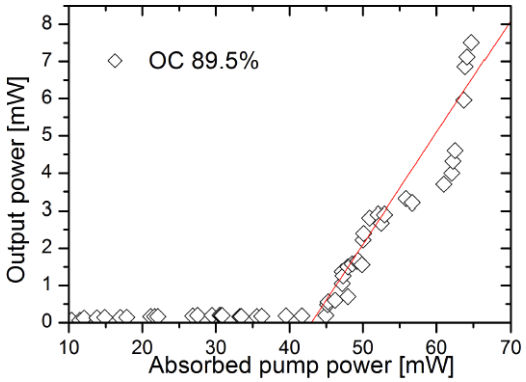

Fig. 6 Dependence of output power on the absorbed pump power using the air–crystal interface as the output coupler

mirror was used (Fig. 6), the estimated loss gives <1 dB/cm. The fact that this value is lower is reasonable because there was no contribution of the crystal-immersion oil–OC interface to the total losses; furthermore, the large difference compared to 8.6 dB/cm allows us to conclude that the waveguide most probably was a different one. Thus, by lowering the waveguide losses in the fabrication process (e.g., lower ion dose, optimized channel width, improvement of the masking technique) and optimizing the neodymium concentration, it might be possible to obtain a shorter laser system with higher efficiency and lower pump threshold in which the OC is the air–crystal interface.

Further work is necessary to eliminate nonuniform physical features during channel waveguide fabrication, thus the masking technique will influence the characteristics of the channels produced. The typical thickness of the metallic mask required to stop ions from an implantation process with the parameters used in this work is around 5 μm. This technical requirement gives rise to a not well-defined boundary in the mask by using standard microlithography, hence with potential influence on propagation losses of the waveguides. Recently, an electroformed mask has been used to form channel waveguides in Nd:YAG by ion implantation [16]; furthermore, laser oscillation was demonstrated on these structures, and they showed single-mode operation [5]. In general, these channel waveguides have shown better performance in comparison with the vanadate waveguides reported in this work, with lower threshold pump powers and propagation loss coefficient. Investigations are underway to use this new masking technique combined with ion implantation to generate channel waveguides in Nd:YVO_4 crystals. The study will involve the fabrication of several channel sets with different width to find the optimum value for low-loss and single-mode waveguides. A commercial laser diode delivering modest 808-nm powers may be used on-chip to pump these waveguides and form in this way an integrated laser device.

4 Conclusion

We have demonstrated and characterized 1064-nm laser oscillation in channel waveguides fabricated by carbon implantation on Nd:YVO_4 using different output couplers. By applying an annealing treatment to the crystal prior to the laser study, the losses were reduced thus improving the waveguide quality. The main results obtained such as ∼9-mW maximum output power, ∼30% slope efficiency, ∼45 mW minimum pump threshold, and lasing without a physical mirror are possible to be improved by addressing issues such as loss minimization, optimal neodymium concentration doping, and reconsidering the masking technique used for waveguide formation. This small laser that operates at room temperature finds potential applications on on-chip fabricated laser-diode-pumped micro-lasers.

Acknowledgements This research was financially supported by CONACyT-Mexico (projects J42695-F, and 52727 and doctoral scholarship 167376). We are thankful to K. López and F. Jaimes for the realization of the implants and to Dr. J.J. Soto for his useful comments.

References

1. C.C. Davis, *Lasers and Electro-Optics: Fundamentals and Engineering*, 1st edn. (University Press, Cambridge, 2000)
2. R. Sundar, K. Ranganathan, A.K. Nath, Opt. Laser Technol. **39**(7), 1426 (2007)
3. S.J. Field, D.C. Hanna, D.P. Shepherd, A.C. Tropper, P.J. Chandler, P.D. Townsend, L. Zhang, IEEE J. Quantum Electron. **27**, 428 (1991)
4. S.J. Field, D.C. Hanna, A.C. Large, D.P. Shepherd, A.C. Tropper, P.J. Chandler, P.D. Townsend, L. Zhang, Electron. Lett. **27**, 2375 (1991)
5. E. Flores-Romero, G.V. Vázquez, H. Márquez, R. Rangel-Rojo, J. Rickards, R. Trejo-Luna, Opt. Express **15**, 17874 (2007)
6. P.P. Yaney, L.G. DeShazer, J. Opt. Soc. Am. **66**, 1405 (1976)
7. P.D. Townsend, P.J. Chandler, L. Zhang, *Optical Effects of Ion Implantation* (Cambridge University Press, Cambridge, 2006)
8. F. Chen, X.-L. Wang, K.-M. Wang, Opt. Mater. **29**, 1523 (2007)
9. M.E. Sánchez-Morales, G.V. Vázquez, P. Moretti, H. Márquez, Opt. Mater. **29**, 840 (2007)
10. M.E. Sánchez-Morales, G.V. Vázquez, H. Márquez, J. Rickards, R. Trejo-Luna, J. Mod. Opt. **53**, 539 (2006)
11. M.E. Sánchez-Morales, Study of optical waveguides in Nd:YVO_4 for the development of compact lasers. Doctoral thesis, CIO, Mexico (2007)
12. M. Young, *Optics and Lasers* (Springer, Berlin, 1992)
13. Y. Nobe, H. Takashima, T. Katsumata, Opt. Lett. **43**, 16 (1217) (1994)
14. F. Chen, L. Wang, Y. Yiang, X.-L. Wang, K.-M. Wang, G. Fu, Q.-M. Lu, Appl. Phys. Lett. **88**, 071123 (2006)
15. E. Lallier, J.P. Pocholle, M. Papuchon, M.P. De Micheli, M.J. Li, Q. He, D.B. Ostrowsky, C. Grezes-Besset, E. Pelletier, IEEE J. Quantum Electron. **27**, 618 (1991)
16. E. Flores-Romero, G.V. Vázquez, H. Márquez, R. Rangel-Rojo, J. Rickards, R. Trejo-Luna, Opt. Express **15**, 8513 (2007)